Lasers in Medical Science (2019) 34:179–190
https://doi.org/10.1007/s10103-018-2680-9

ORIGINAL ARTICLE

The retinal pigment epithelial response after retinal laser photocoagulation in diabetic mice

Sun Young Jang[1,2] · In Hwan Cho[2,3] · Jin Young Yang[4,5] · Ha Yan Park[4] · Sang Earn Woo[1] · Sanjar Batirovich Madrakhimov[4] · Hun Soo Chang[4,5] · Jungmook Lyu[6] · Tae Kwann Park[1,2,4,5]

Received: 20 August 2018 / Accepted: 31 October 2018 / Published online: 29 November 2018

Abstract

To investigate the characteristics of regenerated retinal pigment epithelial (RPE) cells after retinal laser photocoagulation in diabetic mice. C57BL/6J mice were used to induce diabetes using intraperitoneal injection of streptozotocin. The proliferation of RPE cells after laser photocoagulation was determined using the 5-ethynyl-2′-deoxyuridine (EdU) assay in both diabetic and wild-type mice. The morphological changes of RPE cells were evaluated by using Voronoi diagram from immunostaining for ß-catenin. Characteristics of regenerated cells were evaluated by quantifying the mRNA and protein levels of RPE and epithelial-mesenchymal transition (EMT) markers. There were significantly less EdU-positive cells in laser-treated areas in diabetic mice than wild-type mice. Hexagonality was extensively lost in diabetic mice. Many EdU-positive cells were co-localized with Otx2-positive cells in the center of the laser-treated areas in wild-type mice, but only EdU-positive cells were widely distributed in diabetic mice. Quantitative analysis of mRNA and protein levels showed that the expression levels of RPE markers, Pax6, Mitf, and Otx2, were significantly decreased in RPE of diabetic mice compared with that of wild-type mice, whereas the expression levels of EMT markers, vimentin and fibronectin, were significantly increased. The proliferation and hexagonality of regenerating RPE cells were impaired after laser photocoagulation, and the regenerated RPE cells lost their original properties in diabetic mice. Further clinical research is needed to elucidate the RPE response after laser photocoagulation in diabetic patients.

Keywords Diabetic mouse · Laser photocoagulation · Retinal pigment epithelium

Introduction

Retinal laser photocoagulation is a well-established therapeutic option for proliferative retinal vasculopathies, including diabetic retinopathy, which is a leading cause of vision loss in developed countries [1]. Since the reports of the Early Treatment Diabetic Retinopathy Study, it has been shown that laser photocoagulation reduces the risk of vision loss by

Sun Young Jang and In Hwan Cho contributed equally to the work presented here and should therefore be regarded as equivalent first authors.

Tae Kwann Park and Jungmook Lyu should be regarded as equivalent corresponding authors.

✉ Jungmook Lyu
lyujm5@gmail.com

✉ Tae Kwann Park
tkpark@schmc.ac.kr

[1] Department of Ophthalmology, Soonchunhyang University Hospital Bucheon, Soonchunhyang University College of Medicine, #170 Jomaru-ro, Bucheon-si, Gyeonggi-do 14584, South Korea

[2] Department of Ophthalmology, College of Medicine, Soonchunhyang University, Cheonan-si, Chungcheongnam-do, South Korea

[3] Department of Ophthalmology, Soonchunhyang University Hospital Cheonan, Cheonan-si, Chungcheongnam-do, South Korea

[4] Research center for clinical medicine, Soonchunhyang University Hospital Bucheon, Bucheon-si, Gyeonggi-do, South Korea

[5] Department of Interdisciplinary Program in Biomedical Science Major, Graduate School, Soonchunhyang University, Bucheon-si, Gyeonggi-do, South Korea

[6] Department of Medical Science, Konyang University, 685 Gasoowon-dong, Seo-gu, Daejeon 302-718, Daejeon, South Korea

proliferative diabetic retinopathy and diabetic macular edema [2–4]. Even though the anti-vascular endothelial growth factor treatment for retinal diseases has become increasingly popular [5], many clinicians still believe retinal laser photocoagulation should have an important role in the treatment of various retinal vasculopathies [6].

The primary target of laser treatment is the retinal pigment epithelial (RPE) layer, located between Bruch's membrane and the photoreceptors [7]. Human RPE cells play several essential roles; the tight junctions between RPE cells form part of the blood retinal barrier that protects the neural retina from substances in the choroidal circulation. The RPE supplies the metabolically active retina with nutrients and oxygen, and removes photo-oxidative debris from rods and cones. RPE cells are invariably hexagonal in shape, but this morphology may be compromised by aging and cell loss [8]. During laser treatment, heat derived from light energy induces photo-thermal effects in the melanosomes of the RPE, triggering loss of RPE cell hexagonality and structural defects in the neural retina and Bruch's membrane [9]. The Bruch's membrane damage may cause the permanent loss of RPE cell hexagonality. In contrast to the irreversible collateral damage occurring around chorioretinal tissues, it has been reported that damage to the RPE layer can be repaired by morphologically heterogeneous populations of regenerated RPE cells [10, 11]. Overall, it is well-known that micro-scale injuries to RPE cells, such as those induced by laser photocoagulation, can induce RPE cell proliferation [12]. Since the RPE layer has many important physiological actions, including maintenance of visual functions and the viability of photoreceptor cells [12], permanent damage to the RPE layer induces photoreceptor cell degeneration and loss of visual function [13]. Ultimately, homeostatic regulation of RPE cell integrity is important to allow restoration of the integrity of the RPE cell layer after damage.

We have previously investigated RPE regeneration after laser treatment in normal mouse eyes [14–16]. As results, we found that the majority of the laser photocoagulation-induced cell proliferation occurred during the first 3 days, and many proliferating cells were identified as inflammatory cells, RPE cells, endothelial cells, and Müller cells [14]. We also found that laser photocoagulation activated *Wnt*/ß-catenin signaling, promoting RPE proliferation, differentiation, and the epithelial-mesenchymal transition (EMT) [15]. Furthermore, we reported the characteristics of the regenerated retinal pigment epithelium after selective retina therapy, which involved a newly developed laser device that was designed to limit laser-induced damage to only the retinal pigment epithelium [16]. We noted selective retinal lesions that were recovered by proliferation of the retinal pigment epithelium present in the treated spot, as well as by expansion of adjacent RPE cells [16].

As mentioned above, retinal laser photocoagulation is a therapeutic option for diabetic retinopathy. Therefore, we believed that it would be clinically useful to investigate changes of the RPE after retinal laser treatment in diabetes. Although human and mouse eyes differ significantly in certain aspects [17], both use similar molecular mechanisms to regulate growth, replication, differentiation, and death [18]. Furthermore, mice have a short generation time and are easy to handle. Thus, mouse models have been widely used in various research fields. There have been a few clinical and experimental studies describing anatomical and physiological changes of the retina in diabetes [16–19]. Maeshima et al. reported that the size of laser scars from laser-induced chorioretinal atrophy continuously increased over a long period in 19 eyes with diabetic retinopathy [19]. It has recently been shown that retinal levels and nuclear translocation of ß-catenin increased, and the canonical *Wnt* pathway was activated, during diabetic retinopathy in human patients and diabetic rat models [20]. Furthermore, the expression of Otx2 was significantly inhibited in a gestational diabetes mellitus animal model [21]. High glucose levels were reported to induce impairment of tight junctions and increase the apoptosis of RPE cells [22]. To date, there has been no comparative study of the RPE response to laser treatment between diabetic and non-diabetic conditions; however, it is important to characterize molecular differences during the proliferation and differentiation of laser-irradiated RPE layers between diabetic and non-diabetic tissues.

In the present study, we investigated the effect of laser photocoagulation in regeneration of RPE cells in streptozotocin (STZ)-induced diabetic mice.

Materials and methods

Animals

A total of 60 healthy C57BL/6J mice (OrientBio, Sungnam, Republic of Korea) were used in this study. The animals were housed in a temperature- and humidity-controlled room with a fixed 12-h light/12-h dark cycle, and were provided with food and water ad libitum. The study was approved by the Animal Care Committee of Soonchunhyang University Bucheon Hospital, and animal treatment and care meticulously followed the dictates of the ARVO Statement for the Use of Animals in Ophthalmic and Vision Research.

Induction of diabetes

Experimental diabetes was induced in 8-week-old C57BL/6 mice by a single intraperitoneal (IP) injection of STZ (150 mg/kg; Sigma-Aldrich, St. Louis, MO, USA). STZ was freshly prepared in 100 mM citrate buffer (pH 4.5). To prevent sudden hypoglycemic shock, the mice were fed 10% sucrose overnight after the IP STZ injection. Induced hyperglycemia was confirmed by measuring blood glucose using the Accu-

Check active blood glucose monitor (Roche Diagnostics, Mannheim, Germany). After 1 month of induction, only mice with non-fasting blood glucose levels > 300 mg/dL, polyuria, or glucosuria were defined as STZ-induced diabetic mice and used in the experiments. Non-diabetic, age-matched C57BL/6 mice were used as the controls. The time course of changing blood glucose and body weights of the STZ-induced diabetic mice are described in Fig. 1.

Laser photocoagulation

The animals were anesthetized by IP injection of a mixture of 40 mg/kg zolazepam/tiletamine (Zoletil; Virbac, CarrosCedex, France) and 5 mg/kg xylazine (Rompun; Bayer Healthcare, Leverkusen, Germany). The pupil was dilated with 0.5% tropicamide and 2.5% phenylephrine (Mydrin-P; Santen, Emeryville, CA, USA) and both eyes of the mice were used for laser photocoagulation. Laser photocoagulation (200 μm spot size, 0.02 s duration, 100 mW laser power) was performed via slit-lamp delivery of the laser from a PASCAL streamline 532 (Topcon Medical Laser Systems, Santa Clara, CA, USA). The laser uses a frequency-doubled neodymium-doped yttrium aluminum garnet (Nd:YAG) laser diode at a wavelength of 532 nm, which is pumped by semiconductor lasers. To render the corneal surface planar, a handheld flat-glass coverslip was used as a contact lens, with application of 0.5% methylcellulose (Genteal; Novartis, East Hanover, NJ, USA) in front of the mouse eyes. Mice were divided into four groups: wild-type mice without (pre-) laser photocoagulation, STZ-induced diabetic mice without (pre-) laser photocoagulation, wild-type mice with laser photocoagulation, and STZ-induced diabetic mice with laser photocoagulation. For immunohistochemistry (IHC) and the 5-ethynyl-2′-deoxyuridine (EdU) assay, 8 or 10 laser spots were distributed around the optic nerve head of the eye in a concentric pattern. For western blotting and real-time polymerase chain reaction (RT-PCR) analysis, 50 laser shots were applied around the optic nerve head. If a lesion produced a gaseous bubble, indicating rupture or hemorrhage of Bruch's membrane, the animal was excluded from the study. Tissues from three mice of each group were subjected to EdU assay and IHC analysis (two groups: laser-treated wild-type and diabetic mice [6 animals]; four groups: wild-type and diabetic mice undergoing laser treatment or not [12 mice] at each of two time points [7 and 30 days], giving a total of 26 mice). Tissues from 3 to 4 mice of each group were subjected to Western blotting and RT-PCT (total: 34 mice).

IP injection of EdU

To detect proliferation of cells induced by laser photocoagulation, IP injection of EdU (10 mg/kg; Invitrogen, Carlsbad, CA, USA) was performed. Mice received an IP injection of EdU in phosphate-buffered saline (PBS) twice a day for 0–7 days and 0–30 days after laser photocoagulation. The animals were sacrificed and the whole mount preparations for EdU assays were performed at 7 and 30 days after laser photocoagulation. The experimental schemes for periodic IP EdU injections from the time of the STZ injection and laser photocoagulation are shown in Fig. 2.

Tissue preparation for whole mounts

Mice were deeply anesthetized with an IP injection of a 4:1 mixture of zolasepam/tiletamine (80 mg/kg, Zoletil; Virbac) and xylazine (10 mg/kg, Rompun; Bayer Healthcare). After anesthesia, intracardial perfusion with 0.1 M PBS containing 1000 U/mL heparin, followed by 4% paraformaldehyde (PFA) in 0.1 M PBS, was performed. The eyeballs of mice were enucleated and the anterior segments, including the cornea, lens, and neural retina, were removed by cutting through the limbal cornea. The RPE-choroid complex was then fixed with 4% PFA in 0.1 M PBS at pH 7.4 for 2 h, and prepared as flattened whole mounts with four equidistant cuts.

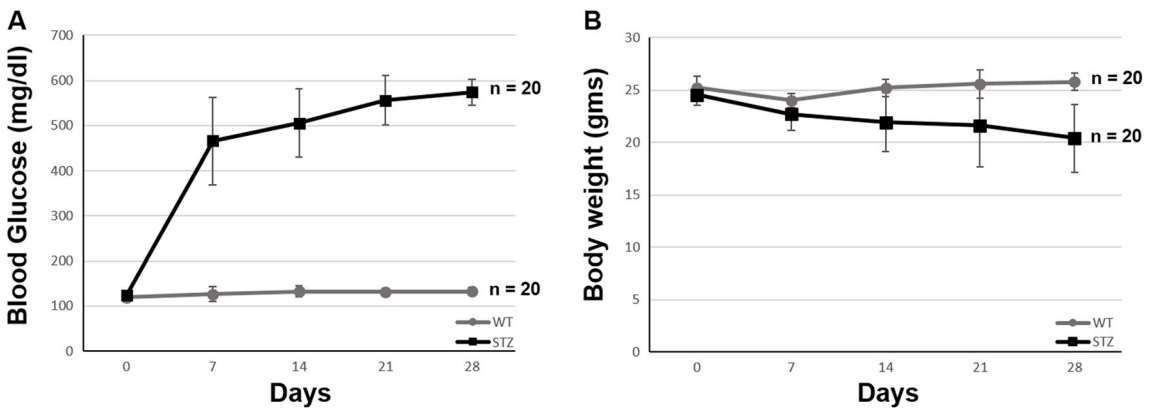

Fig. 1 Changes in blood glucose levels and body weights of wild-type and STZ-induced diabetic mice. STZ, streptozotocin

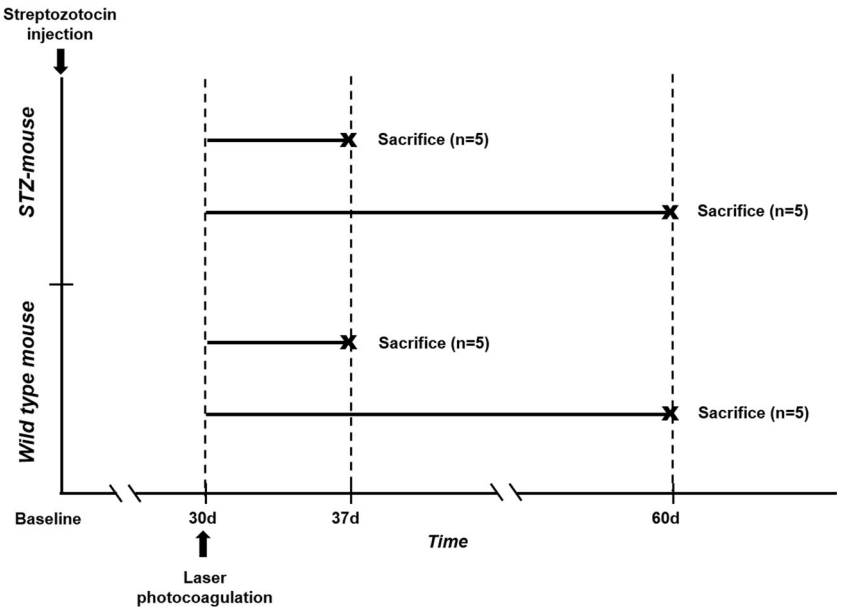

Fig. 2 Schematics of the protocols for periodic IP EdU injections from the time of STZ injection and laser photocoagulation (arrows). The mice received an IP injection of EdU in phosphate-buffered saline twice a day for 0–7 days and 0–30 days after laser photocoagulation. The mice were euthanized at the end of each injection period. IP, intraperitoneal; EdU, 5-ethynyl-2′-deoxyuridine; STZ, streptozotocin

EdU assay

EdU incorporation into DNA was detected using a commercial EdU imaging kit (Click-iT EdU Alexa Fluor 647 imaging kit; Invitrogen) by following the manufacturer's protocol. All procedures of the Click-iT reaction were performed at room temperature. The samples were permeabilized in 1.0% Triton X-100 for 20 min and rinsed three times in PBS, for 10 min per rinse. The EdU cocktail including the reaction buffer, $CuSO_4$, azide, and buffer were added for 30 min, as per the manufacturer's protocol, and rinsed three times in PBS for 15 min per rinse. The azide was coupled to Alexa Fluor 647. The images were obtained at each time point after laser photocoagulation using confocal fluorescence microscopy (LSM510 META; Carl Zeiss, Jena, Germany).

Immunostaining analysis

The samples were washed three times for 15 min each with 0.1% Triton X-100 in PBS (PBST; Sigma-Aldrich) and blocked with 5% goat serum in PBST for 1 h at room temperature. After blocking, the samples were incubated with primary antibodies including anti-ß-catenin antibody (1:200, C7207; Sigma-Aldrich), anti- Otx2 antibody (1:200, sc-30,659; Santa Cruz Biotechnology, Santa Cruz, CA, USA), and anti-vimentin antibody (1:200, ab92547; Abcam, Cambridge, UK) overnight at 4 °C. On the next day, the samples were incubated with secondary antibodies for 2 h at room temperature.

For double immunostaining with EdU and Otx2, the whole mount was washed for 3 min in PBS and blocked for 30 min using 5% goat serum in PBST. Anti-Otx2 antibody (1:200, sc-30,659; Santa Cruz Biotechnology) was then added for an overnight incubation at 4 °C in the same solution. The next day, the tissue was washed several times and secondary antibody was added for 2 h at room temperature. After the tissue was washed for 10 min using 3% bovine serum albumin in PBS, the Click-iT EdU imaging kit was used to prepare the Click-iT reaction cocktail reagent, and the tissue was incubated for 30 min. Images were obtained at each time point after laser photocoagulation using confocal fluorescence microscopy (LSM710; Carl Zeiss). Alexa Fluor-488 anti-rabbit (1:1000, 11,034; Thermo Fisher Scientific, Waltham, MA, USA), Alexa Fluor-488 anti-mouse (1:1000, A11031; Thermo Fisher Scientific), and Alexa Fluor-568 anti-goat (1:1000, A11055; Thermo Fisher Scientific) antibodies were used as the secondary antibodies.

Western blot analysis

The expression level of Otx2 and EMT markers, such as vimentin and fibronectin, in the RPE-choroid complex was analyzed by western blotting. Mice were anesthetized and perfused intracardially with 10 mL cold Dulbecco's PBS (DPBS; pH 7.0). After enucleation of the right eyeball, the cornea, lens, and neural retina were removed, and 100 μL lysis buffer was added to the RPE-choroid complex. Tissue extracts were sonicated, placed on ice for 50 min, and then centrifuged (17,000×*g*, 20 min, 48 °C). The supernatant was collected and the protein concentration in the homogenate was measured using a Pierce BCA protein assay kit (Thermo Scientific, Rockford, IL, USA) following the manufacturer's protocol. An equal volume of total protein (7.5 μg) from each extract was resolved by sodium dodecyl sulfate-polyacrylamide gel electrophoresis (SDS-PAGE) and transferred to nitrocellulose membranes (0.2 μm pore size;

Amersham Protan, GE Healthcare Life Sciences, Marlborough, MA, USA) The membranes were blocked with 5% skim milk for 1 h at room temperature and incubated with anti-Otx2 (1:200, sc-30,659; Santa Cruz Biotechnology), anti-vimentin (1:1000, ab92547; Abcam), and anti-fibronectin (1:500, ab45688; Abcam) antibodies overnight at 48 °C. Subsequently, the membrane was incubated with goat anti-rabbit IgG (H + L)-horseradish peroxidase-conjugated secondary antibody (1:1000, SA002-500; Gendepot, Houston, TX, USA) for 2 h at room temperature. The blot was developed using the enhanced chemiluminescence system (West-Q Pico ECL solution; Gendepot), and densitometry of the bands was performed by drawing the regions of the bands of interest. Band intensities were quantified using ImageJ software (National Institutes of Health, Bethesda, MD, USA (in the public domain) and were averaged from five samples.

RNA isolation and RT-PCR analysis

The mRNA levels of RPE-specific transcriptional factors, such as Pax6, Mitf, and Otx2 were measured by quantitative RT-PCR. Total mRNA was prepared from the RPE-choroid complex using TRIzol reagent (Invitrogen, Tokyo, Japan). The mRNA (0.5~1 μg) was reverse-transcribed using Superscript III (Invitrogen). Quantitative RT-PCR was conducted using a SYBR Green kit (Philekorea, London, UK), and the samples were quantified by amplifying *Gapdh* as an internal control for each sample. The PCR amplification was performed using specific primer pairs, as listed in Table 1.

Cell counting

The numbers of positive Edu and/or Otx2 cells were estimated on laser photocoagulated whole mount RPE-choroid complexes. Cell counting was performed manually by three independent, experienced researchers who were blinded to the identity of each sample. Five laser-treated lesions showing typical morphology were selected and averaged from each animal for quantitative analyses. The Edu-positive and/or Otx2-positive cells within circles of 100 μm, 200 μm, 100–200 μm, and 200–300 μm were counted separately at 7 and 30 days after laser photocoagulation to evaluate location-dependent changes in the number of cells.

Voronoi diagram

To evaluate the variation in morphology of the RPE cells between wild-type and STZ-induced diabetic mice at each time point (prelaser photocoagulation at 7 and 30 days after laser photocoagulation), the Voronoi diagram algorithm program (Rhinoceros 5.0; Roberts McNeel, Seattle, WA, USA) was used for analysis of ß-catenin-stained RPE cells.[20] The RPE cells with intact ß-catenin staining in five laser-treated mouse retinas were averaged for the analysis. The hexagonality and coefficients of variance of the areas of the RPE cells stained with ß-catenin, within circles 200 μm in diameter, were estimated and calculated using ImageJ software (National Institutes of Health).

Image and statistical analyses

Statistical analyses were conducted using SPSS for Windows statistical software (ver. 20.0; SPSS Inc., Chicago, IL, USA). The Wilcoxon signed-rank test was used to compare wild-type and STZ-induced diabetic mice at each time point. A value of $p < 0.05$ was considered to indicate statistical significance for the Wilcoxon signed-rank test. The Kruskal-Wallis test with post hoc analysis was used for multiple comparisons among each time point. All quantified values are expressed as means ± SEM. A value of $p < 0.016$ was considered to indicate statistical significance after Bonferroni correction.

Results

RPE cell proliferation after laser photocoagulation

To determine the proliferative activity of RPE cells in laser-treated areas, the EdU assay was performed. The number of EdU-positive cells were counted in one microscopic field in the laser-treated areas in retinas of wild-type mice and diabetic mice at each time point (7 and 30 days after laser

Table 1 List of primers used for PCR

Gene	Primer sequence	
	Forward	Reverese
Pax6	5'-GTCAGTGAATGGGCGGAGTT-3'	5'-ACTTGGACGGGAACTGACAC-3'
Mitf	5'-AACTGCAGCCAGGAACTTGT-3'	5'-CGGTGACTCCAACAGGTGAG-3'
Otx2	5'-ACAAGTGGCCAGTTCAGTCC-3'	5'-CCATGCCCCCAAAGTAGGAA-3'
Gapdh	5'-ACGGCAAATTCAACGGCACAG-3'	5'-GGTCATGAGCCCTTCCACAAT-3'

photocoagulation). At 7 days after laser photocoagulation, the number EdU-positive cells was significantly increased in diabetic mice compared with wild-type mice (28.6 ± 7.1 vs. 38.6 ± 13.9 cells/field, $p = 0.002$) (Fig. 3a, b, e). However, at 30 days after laser photocoagulation, there were significantly fewer EdU-positive cells in diabetic mice than wild-type mice (41.7 ± 8.3 vs. 53.3 ± 9.8 cells/field, $p = 0.030$) (Fig. 3c–e). In wild-type mice, EdU-positive cells were significantly increased at 30 days compared to 7 days after laser photocoagulation (28.6 ± 7.1 vs. 53.3 ± 9.8 cells/field, $p = 0.001$) (Fig. 3a, c, ,e). However, in diabetic mice, EdU-positive cells were not significantly increased at 30 days compared to 7 days after laser photocoagulation (38.6 ± 13.9 vs. 41.7 ± 8.3 cells/field, $p = 0.687$) (Fig. 3b, d, e).

RPE cell morphology after laser photocoagulation

To evaluate the morphological changes of RPE cells after laser photocoagulation, RPE whole mounts from the eyes of wild-type and diabetic mice were immunostained with ß-catenin antibody to assess the hexagonality of RPE cells. Before laser treatment, the hexagonality of the retinal pigment epithelium in diabetic mice was the same as that in wild-type mice (Fig. 4a). However, at 7 days after laser application, the hexagonality of the RPE cells in diabetic mice was more extensively lost compared to wild-type mice. Furthermore, until 30 days after laser photocoagulation, the hexagonality of the RPE cells was more extensively lost in diabetic mice compared to wild-type mice (Fig. 4a). In addition, the fluorescence signals of ß-catenin revealed that nuclear or cytoplasmic ß-catenin was detected more frequently in cells exhibiting loss of hexagonal shape than in hexagonal RPE cells.

To objectively assess the hexagonality of RPE cells, we evaluated variations in the sizes of RPE cells, areas of individual RPE cells using Voronoi diagrams, and a coefficient of variance (CV) within a 200-μm circle of the laser-treated areas at different time points, in wild-type and diabetic mice (prelaser photocoagulation, 7 and 30 days after laser photocoagulation) (Fig. 4b). The hexagonality of RPE cells significantly decreased (day 7, $p = 0.001$; day 30, $p < 0.001$) and the CV of RPE cell areas significantly increased (day 7, $p < 0.001$; day 30, $p < 0.001$) in diabetic mice compared to wild-type mice at 7 and 30 days after laser photocoagulation (Fig. 4c, d).

Quantitative evaluation of EdU/Otx2 double-positive cells after laser photocoagulation

To determine whether the proliferating cells took on characteristics specific to RPE cells, and to characterize the distribution patterns of these cells, RPE whole mounts from wild-type and diabetic eyes were immunostained with Otx2 and EdU antibodies and then the numbers of EdU/Otx2 double-positive cells in different regions were counted (area I, within a circle < 100 μm; area II, 100–200 μm; and area III, 200–300 μm; Fig. 5a). Area I was the arbitrary area that was directly hit by the laser, and areas II and III were located at increasing distances from the center of the laser-treated area.[9]

In wild-type mice, many Otx2-positive cells were positive for EdU, especially in the center of laser-treated areas at 7 and 30 days after laser photocoagulation (Fig. 5a, c). However, in diabetic mice, a few EdU/Otx2 double-positive cells was

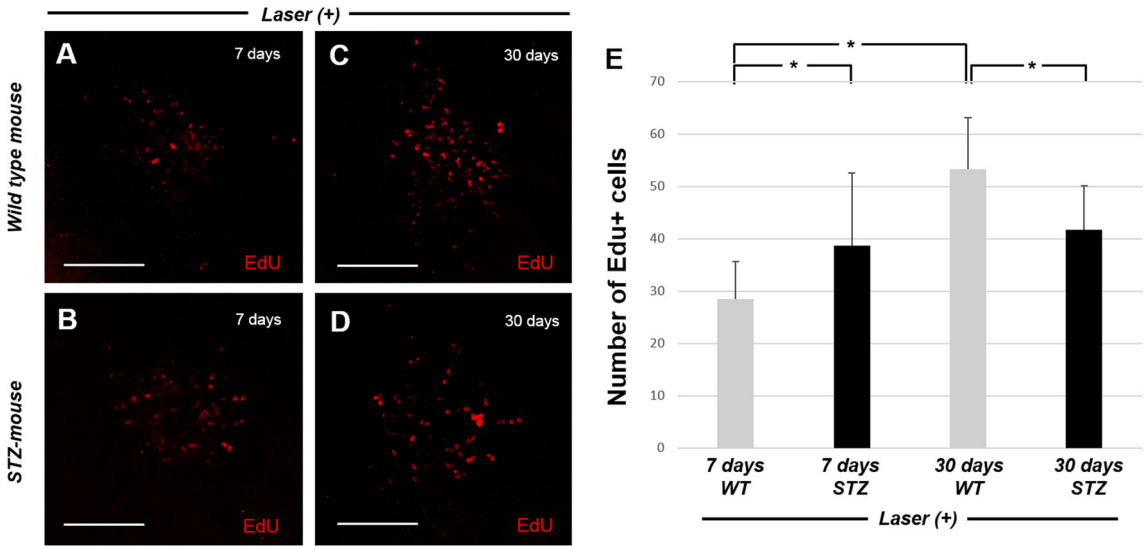

Fig. 3 The EdU expression in laser-treated lesions in wild-type and STZ-induced diabetic mice at 7 days and 30 days after laser photocoagulation. **a**, **b**, **e** At 7 days after laser photocoagulation, there were significantly more EdU-positive cells in STZ-induced diabetic than wild-type mice. **c**, **d**, **e** However, at 30 days after laser photocoagulation, EdU-positive cells were not significantly increased in STZ-induced diabetic mice and were significantly less abundant than in wild-type mice. STZ, streptozotocin; Edu, 5-ethynyl-2′-deoxyuridine. Scale bar: 100 μm. *Significantly different

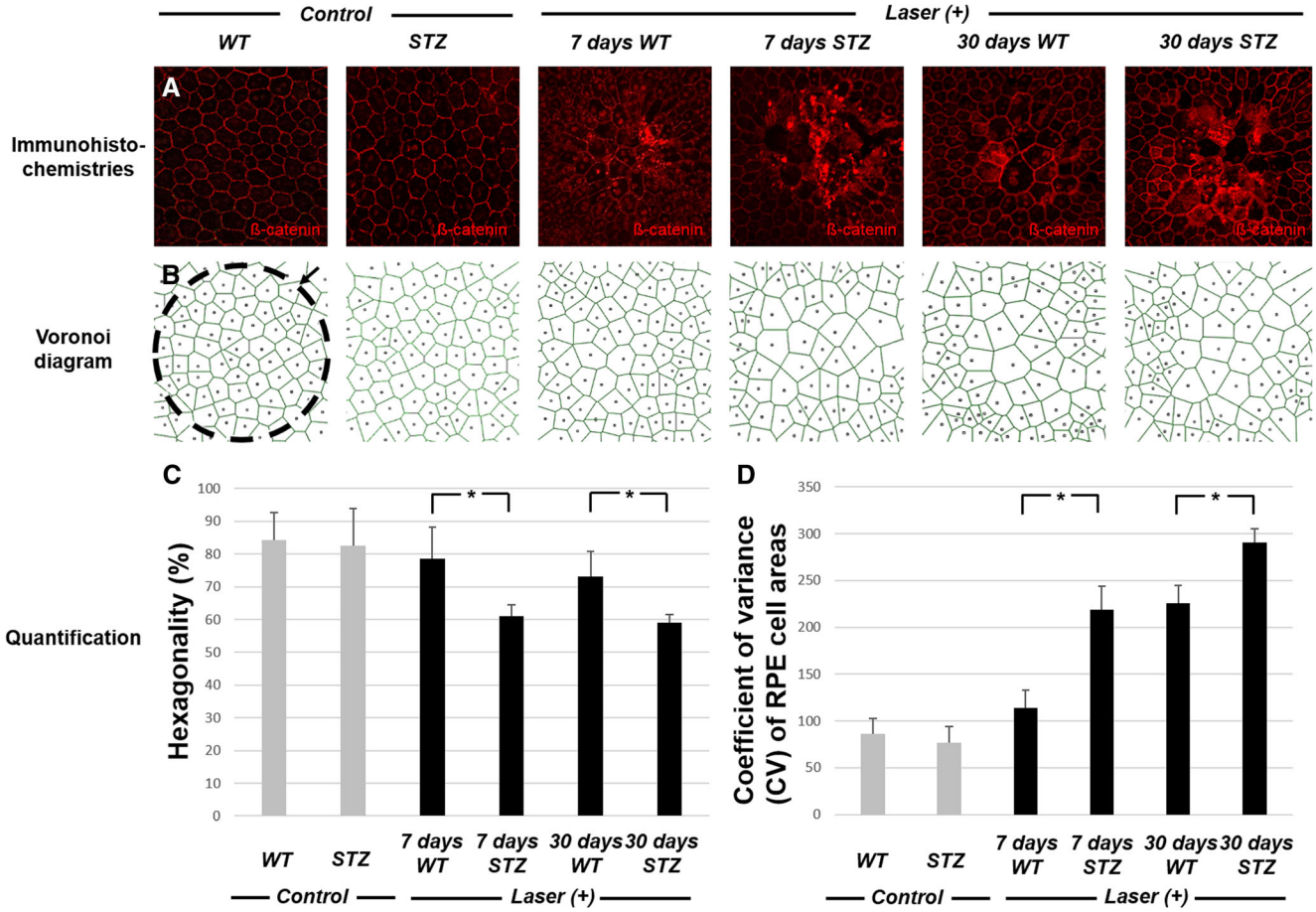

Fig. 4 **a**, **b** Hexagonality and CV of RPE cell areas using a Voronoi diagram within a circle 200 μm (arrow) at prelaser photocoagulation, 7 and 30 days after laser photocoagulation. **c**, **d** At 7 and 30 days after laser photocoagulation, the hexagonality of RPE cells significantly decreased ($p = 0.001$ and $p < 0.001$, respectively) and the CV of RPE cell areas significantly increased ($p < 0.001$ and $p < 0.001$, respectively) in STZ-induced diabetic mice compared to wild-type mice. RPE, retinal pigment epithelial; CV, coefficient of variance; STZ, streptozotocin. Scale bar: 100 μm, *Significantly different

detectable and only EdU-positive cells were distributed in the center of laser-treated areas at 7 and 30 days after laser photocoagulation (Fig. 5b, d). In wild-type mice, the numbers of EdU-positive and EdU/Otx2 double-positive cells were significantly decreased with increasing distance (day 7, $p < 0.001$ and $p < 0.001$, respectively; day 30, $p < 0.001$ and $p < 0.001$, respectively), whereas Otx2-positive cells were significantly increased with increasing distance (day 7, $p < 0.001$ and, $p < 0.001$, respectively; day 30, $p < 0.001$ and $p < 0.001$, respectively) from the center of the laser-treated area at 7 and 30 days after laser photocoagulation. In diabetic mice, the number of EdU-positive and EdU/Otx2 double-positive cells in area II was significantly greater than in area I (day 7, $p < 0.001$ and $p < 0.001$, respectively; day 30, $p < 0.001$ and $p = 0.013$, respectively). In area III, the numbers of EdU-positive and EdU-positive/Otx2-positive cells were significantly reduced versus area I (day 7, $p < 0.001$ and $p < 0.001$, respectively; day 30, $p < 0.001$ and $p < 0.001$, respectively), whereas there were significantly more Otx2-positive cells than in area I (day 7, $p < 0.001$ and $p < 0.001$, respectively; day 30, $p < 0.001$ and $p < 0.001$, respectively). In diabetic mice, the numbers of EdU-positive and EdU-positive/Otx2-positive co-localized cells in areas I and III were significantly lower than in wild-type mice at 7 and 30 days after laser photocoagulation (day 7, $p < 0.001$ and $p < 0.001$, respectively, for area I; $p = 0.003$ and $p < 0.001$, respectively, for area III; day 30; $p < 0.001$ and $p < 0.001$, respectively, for area I; $p < 0.003$ and $p = 0.027$, respectively, for area III). The number of Otx2-positive cells was also significantly less than in wild-type mice in area I at 7 and 30 days after laser photocoagulation (day 7, $p < 0.001$; day 30; $p = 0.047$) (Fig. 5e, f, g).

Expression of Pax6, Mitf, and Otx2 after laser photocoagulation

Immunostaining with Otx2 antibody from whole mount preparations revealed that Otx2-positive cells were expressed in the center of laser-treated areas at 7 and 30 days after laser photocoagulation in wild-type mice. However, in diabetic mice, Otx2-positive cells were mainly expressed around the

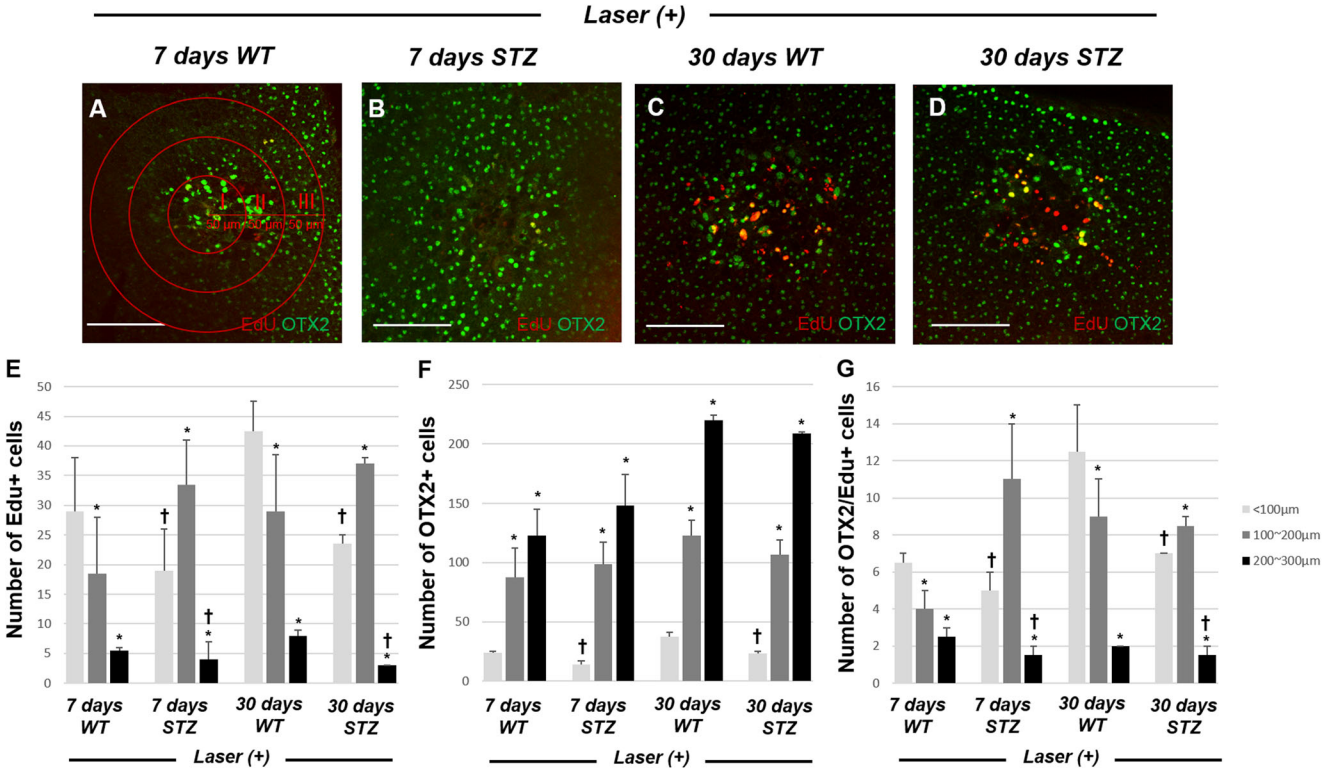

Fig. 5 Immunostaining of EdU-positive and Otx2-positive cells from whole mount preparations in wild-type and STZ-induced diabetic mice at 7 and 30 days after laser photocoagulation. **a**–**d** Many EdU-positive cells were co-localized with Otx2-positive cells in wild-type mice but not in STZ-induced diabetic mice. Only EdU-positive cells were mainly distributed in the center of laser-treated areas in STZ-induced diabetic mice. **e**–**g** EdU-positive cells were mainly distributed in area I in wild-type mice, and in area II in STZ-induced diabetic mice, after laser photocoagulation. The number of Otx2-positive cells increased with increasing distance from the center of the laser-treated area (day 7, $p < 0.001$ and $p < 0.001$, respectively; day 30, $p < 0.001$ and $p < 0.001$, respectively). EdU-positive/Otx2-positive cells were mainly distributed in area I in wild-type mice, and in area II in STZ-induced diabetic mice. EdU, 5-ethynyl-2′-deoxyuridine; STZ: streptozotocin. *Significantly different from area I, †significantly different from wild-type mice. Scale bar: 100 μm

laser-treated areas and barely expressed in the center of laser-treated areas at 7 and 30 days after laser photocoagulation (Fig. 6a–d). Western blot analysis to compare the Otx2 protein levels between the two groups showed that at 30 days after laser photocoagulation in diabetic mice, expression of Otx2 was significantly decreased compared to 7 days after laser photocoagulation ($p = 0.001$) and significantly lower than in wild-type mice ($p < 0.001$; (Fig. 6e).

We quantitated the mRNA levels of RPE-specific transcription factors, such as *Pax6*, *Mitf*, and *Otx2*, using quantitative RT-PCR (Fig. 6f). In wild-type mice, the mRNA levels of *Pax6*, *Mitf*, and *Otx2* were significantly increased at 7 and 30 days after laser photocoagulation compared to prelaser photocoagulation (day 7, $p < 0.001$, $p < 0.001$ and $p < 0.001$, respectively; day 30, $p < 0.001$, $p < 0.001$ and $p < 0.001$, respectively). In diabetic mice, the mRNA levels of *Pax6* and *Otx2* were significantly increased at 7 and 30 days after laser photocoagulation compared to prelaser photocoagulation (day 7, $p = 0.010$ and $p = 0.006$, respectively; day 30, $p = 0.001$ and $p < 0.001$, respectively). In contrast, the mRNA levels of *Mitf* were significantly decreased at 7 days and 30 days after laser photocoagulation compared to prelaser photocoagulation (day 7, $p = 0.039$; day 30, $p = 0.001$). Notably, mRNA levels of *Pax6*, *Mitf*, and *Otx2* were significantly lower in diabetic mice than wild-type mice at every time point (day 7, $p < 0.001$, $p < 0.001$ and $p < 0.001$, respectively; day 30, $p < 0.001$, $p < 0.001$ and $p < 0.001$, respectively) (Fig. 6f).

The EMT after laser photocoagulation

To examine the activity of the EMT in wild-type and diabetic mice after laser photocoagulation, we measured protein levels of EMT markers, such as vimentin and fibronectin, using western blot analysis. The protein levels of vimentin and fibronectin were significantly increased at 7 days after laser photocoagulation compared to prelaser photocoagulation in both wild-type and diabetic mice (wild-type mice, $p < 0.001$ and $p < 0.001$, respectively; diabetic mice, $p < 0.001$ and $p < 0.001$, respectively). The vimentin and fibronectin expression levels were significantly higher in diabetic mice than wild-type mice at 7 and 30 days after laser photocoagulation (day 7, $p = 0.024$ and $p = 0.011$, respectively; day 30, $p < 0.001$ and $p = 0.001$, respectively) (Fig. 7).

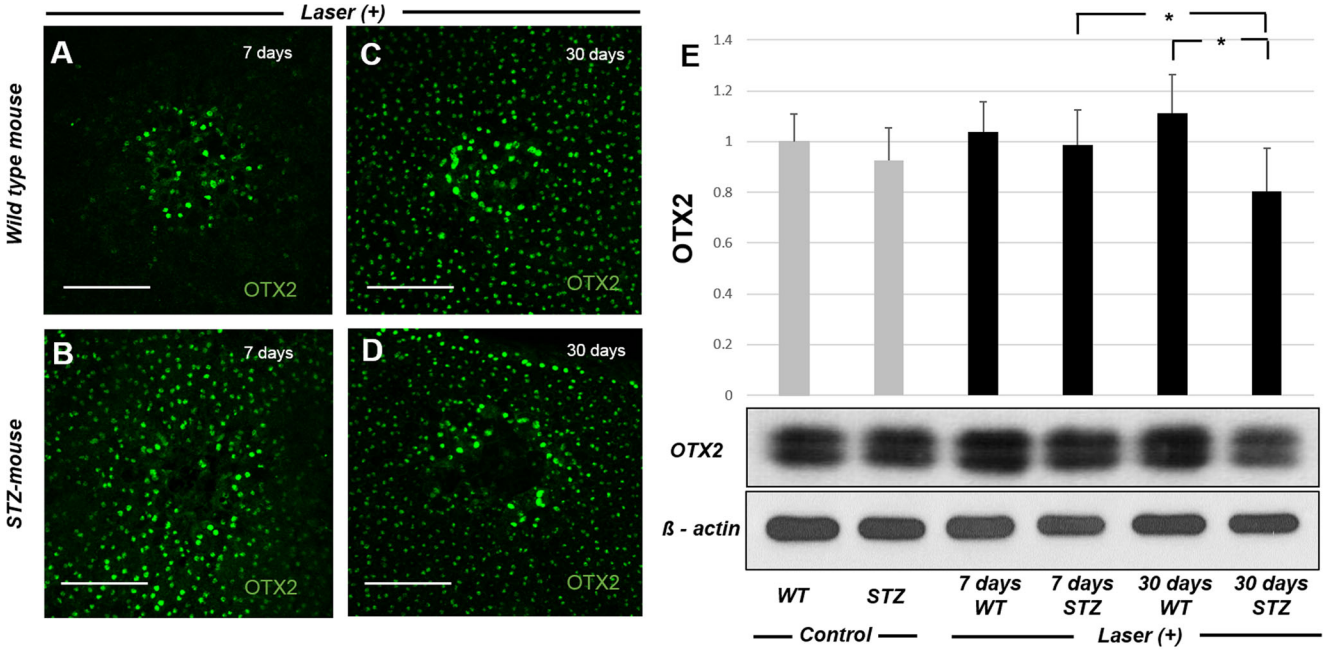

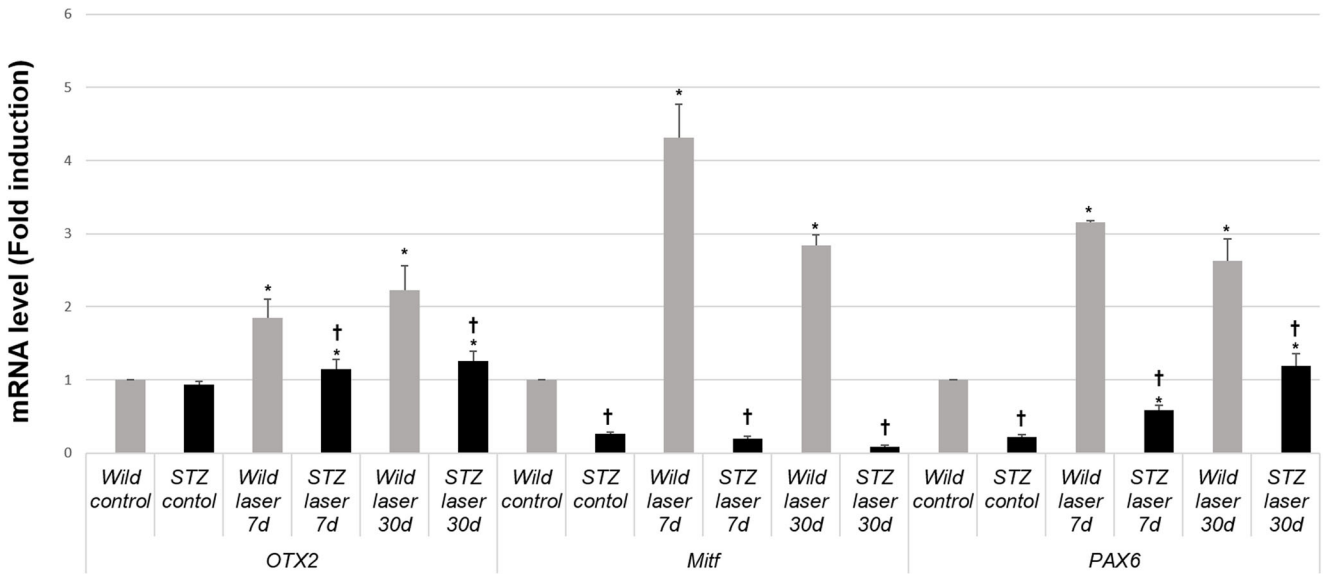

	OTX2	Mitf	PAX6
Wild control	1	1	1
STZ control	0.930482	0.266236	0.226624
Wild laser 7d	1.854079	4.309829	3.15228
STZ laser 7d	1.144188	0.200008	0.584658
Wild laser 30d	2.223066	2.843299	2.631054
STZ laser 30d	1.260328	0.091378	1.194847

Fig. 6 tnostaining of Otx2-positive cells from whole mount preparations in wild-type and STZ-induced diabetic mice at 7 and 30 days after laser photocoagulation. **a**, **c** Wild-type mice; **b**, **d** diabetic mice; **e** mean band intensities from Western blot analyses calculated using ImageJ software for Otx2. At 30 days after laser photocoagulation in diabetic mice, expression of Otx2 was significantly decreased when compared with 7 days after laser photocoagulation, and was significantly lower than in wild-type mice. **f** The mRNA levels of Pax6, Mitf, and Otx2 at different time points in wild-type and STZ-induced diabetic mice. The mRNA levels of Pax6, Mitf, and Otx2 were significantly lower in STZ-induced diabetic mice than wild-type mice at every time point (day 7; $p < 0.001$, $p < 0.001$ and $p < 0.001$, respectively; day 30, $p < 0.001$, $p < 0.001$ and $p < 0.001$, respectively). The mRNA level of Mitf was significantly decreased at 7 and 30 days after laser photocoagulation compared to prelaser photocoagulation (day 7, $p = 0.039$; day 30, $p = 0.001$). STZ, streptozotocin; control, prelaser photocoagulation; laser 7d, at 7 days after laser photocoagulation; laser 30d, at 30 days after laser photocoagulation. *Significantly different from baseline (wild-type control, STZ control); †significantly different from wild-type mice. Scale bar: 100 μm

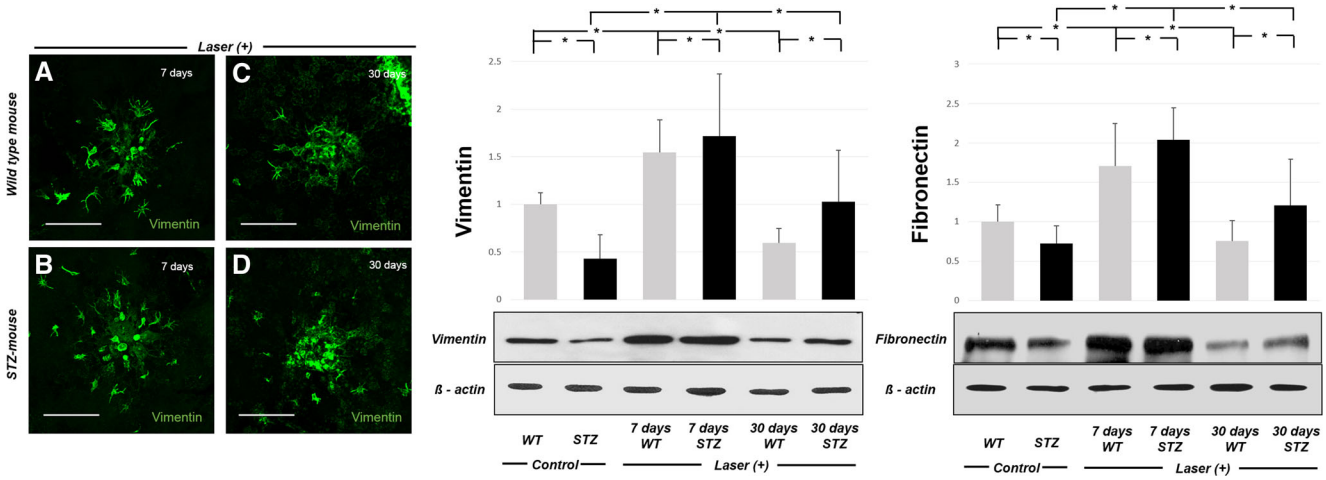

Fig. 7 The protein levels of vimentin and fibronectin in wild-type and diabetic mice at different time points. The vimentin and fibronectin levels were significantly higher in diabetic mice than wild-type mice after laser photocoagulation. STZ, streptozotocin; control, prelaser photocoagulation; laser 7d, at 7 days after laser photocoagulation; laser 30d, at 30 days after laser photocoagulation. *Significantly different from baseline (wild-type control, STZ control); †significantly different from wild-type mice. Scale bar: 100 μm

Discussion

The main target of laser photocoagulation is the RPE layer. Recent studies have focused on changes in the retina pigment epithelium after laser photocoagulation, describing many details of the morphological and biological responses to laser treatment [10, 11, 23, 24]. However, there has been no study investigating the RPE response to laser treatment using diabetic mouse eyes. Because laser photocoagulation has been a therapeutic option for diabetic retinopathy, it is important to investigate its molecular aspects during the proliferation and differentiation of laser-irradiated RPE layers during diabetes. In the present study, we compared regenerated RPE cells after laser photocoagulation from diabetic mice to those of normal control mice.

First, we found that there were significantly less EdU-positive cells in laser-treated areas in diabetic mice compared to wild-type mice. Hexagonality of re-established cells after laser photocoagulation was more extensively lost in diabetic mice. During laser treatment, laser light energy is converted into heat energy, leading to photo-thermal damage of the retinal pigment epithelium [9, 25]. It has been reported that the damaged RPE layer was able to be reestablished by morphologically heterogeneous populations of regenerated RPE cells [10, 11], showing that micro-scaled injury to RPE cells, such as laser photocoagulation, can induce RPE cell restoration [12]. However, in diabetes, the process of wound healing is impaired compared to normal conditions [26]. Even though the process of wound healing in the retina is not well-established, the process of wound healing in the skin has been widely investigated. Over 100 known physiological factors contribute to wound healing deficiencies in patients with diabetes [26]. The wound healing process in the skin is a cellular response to injury that induces activation of keratinocytes, fibroblasts, and endothelial cells. The present study showed for the first time that the cell proliferative potential, involving restoration of hexagonality of RPE cells around the laser site in diabetic mice eyes, was impaired compared to normal mouse eyes. These results suggested that the reestablished RPE cells may lose their original (hexagonal) morphology and changes of the cell signaling pathway might influence the phenotype of reestablished RPE cells in diabetic mice after laser photocoagulation.

Villarroel et al. characterized the effect of high glucose concentration on the permeability and expression of tight junction proteins in a human RPE cell line, and reported that high glucose concentration impaired permeability in RPE cells [22]. Diabetes results from not only high blood glucose levels, but also in association with other factors, such as cytokines, growth factors, reactive oxygen species, and advanced glycation endproducts [27]. Busik et al. reported that diabetes-related endothelial injury in the retina may be due to the release of cytokines induced by glucose, rather than being a direct effect of high glucose [28]. Stojadinovic et al. performed molecular analyses of biopsy tissue from the epidermis of patients with chronic ulcers and reported overexpression of c-myc and nuclear localization of β-catenin in diseased tissue [29]. Notably, they showed that stabilization of nuclear β-catenin inhibited wound healing and keratinocyte migration by blocking the epidermal growth factor response. In the present study, immunostaining of RPE cells for ß-catenin showed an increase in the number of cells displaying nuclear or cytoplasmic ß-catenin expression and loss of their regular hexagonal shape in diabetic mice compared to wild-type mice. These results suggest a possibility that laser photocoagulation may enhance activation of *Wnt/ß-catenin* signaling in diabetic retinopathy. Further study is necessary to determine the molecular mechanism of *Wnt/ß-catenin* signaling in the wound healing process of the retina after laser photocoagulation.

Using laser photocoagulation, the *Wnt*/ß-catenin signaling pathway was activated and subsequently upregulated Otx2 and Mitf, which are key transcriptional factors in RPE formation and EMT markers, such as vimentin, and α-SMA [15]. Importantly, EdU-positive proliferating cells were co-localized with Otx2- and Mitf-positive cells, suggesting that many of the proliferating cells retained a RPE cell-like phenotype [15]. In the present study in wild-type mice, re-established cells in the center of laser-treated area expressed characteristics of RPE cells. However, in diabetic mice, re-established cells in the center of laser-treated area lost some of the original characteristics of RPE cells. Edu-positive proliferating cells that co-localized with Otx2-positive cells were significantly reduced in number in diabetic mice versus wild-type mice after laser photocoagulation. Furthermore, mRNA expression levels of Pax6, Mitf, and Otx2 were significantly lower in diabetic mice than wild-type mice after laser photocoagulation. Pax6 has recently been reported to regulate melanogenesis in the retinal pigment epithelium through regulatory interactions with Mitf [30]. Mitf is also reported to have an important role in maintaining RPE cells via promoting melanin pigment synthesis and regulating cell proliferation [31], and Otx2 has been reported to be a key regulatory transcription factor for RPE specification and differentiation [32, 33]. Because these transcriptional factors are supposed to be expressed sequentially in the process of RPE development, the results of the present study indicated that regenerated cells after laser photocoagulation in the retina of diabetic mice might not have RPE characteristics. Additionally, the EMT activity after laser photocoagulation was compared between diabetic and wild-type mice. The EMT is a process by which epithelial cells lose their cell polarity to become multipotent stromal cells that can differentiate into a variety of cell types [34]. In this study, we found that vimentin and fibronectin, both EMT markers, were upregulated after laser photocoagulation, consistent with previous reports [15]. Western blot analysis revealed that the activity of EMT was significantly increased in diabetic mice compared to wild-type mice after laser photocoagulation. Taken together, we assumed that the re-established cells after laser photocoagulation in diabetic mice did not have RPE characteristics and were transdifferentiated to different kinds of cells by the EMT process.

As we explored the characteristics of regenerated RPE cells after retinal laser photocoagulation only in diabetic mice, we cannot extend our conclusions to humans. Mouse and human cells use similar molecular mechanisms to regulate growth, replication, differentiation, and death. Thus, mouse models have been widely used in various research fields [18]. However, mice are not like humans [17]. The mouse eye has a relatively large cornea and lens; the latter accounts for 60% of the axial length. The mouse retina is rod-dominant and does not have a fovea centralis. Furthermore, the basal metabolic rate per gram of body weight is seven-fold greater in mice than humans [18]. However, molecular changes in RPE cells cannot easily be tracked in human patients, so the use of mouse models is mandatory.

Today, the retinal pigment epithelium can be visualized in some patients using adaptive optics, such as those afforded by scanning laser ophthalmoscopy [35, 36]. It is possible to explore morphological changes in RPE cells (such as decreased hexagonality) after retinal laser photocoagulation in human. Fundus autofluorescence assesses light emission from lipofuscin within RPE cells, and can be used to identify biochemical changes in patients' eyes [37, 38]. Time-resolved autofluorescence reliably identifies not only lipofuscin, but also phenylalanine, tyrosine, tryptophan, NADH, hemoglobin, melanin, collagen, elastin, lutein, and zeaxanthin [38]. Time-resolved autofluorescence can also be used to measure biomarkers of oxidative stress [37]. We believe that clinical research on such advanced imaging modalities will increase our understanding of the reactions of human RPE cells to retinal laser treatment in human.

In conclusion, the proliferation and hexagonality of regenerated RPE cells were impaired after laser photocoagulation, and the regenerated RPE cells lost their original properties in diabetic mice. Changes in RPE-specific transcription factors during diabetes might be involved in such changes. Further clinical study using advanced imaging modalities such as time-resolved autofluorescence will be necessary to elucidate the RPE response after laser photocoagulation in diabetic patients.

Funding information This study was supported by grants from the Basic Science Research Program through the National Research Foundation of Korea (NRF) (No. 2016R1A2B4008376; Seoul, Republic of Korea). This work was partially supported by the Soonchunhyang University Research Fund. The funding organization had no role in the design or conducted of this research.

Compliance with ethical standards

Conflict of interest The authors declare that they have no conflict of interest.

Ethics approval The Animal Care Committee of Soonchunhyang University Bucheon Hospital.

References

1. Prokofyeva E, Zrenner E (2012) Epidemiology of major eye diseases leading to blindness in Europe: a literature review. Ophthalmic Res 47:171–188
2. Preliminary report on effects of photocoagulation therapy (1976) The diabetic retinopathy study research group. Am J Ophthalmol 81:383–396
3. Photocoagulation treatment of proliferative diabetic retinopathy: the second report of diabetic retinopathy study findings (1978). Ophthalmology 85:82–106

4. Photocoagulation treatment of proliferative diabetic retinopathy. Clinical application of Diabetic Retinopathy Study (DRS) findings, DRS Report Number 8 (1981) The diabetic retinopathy study research group. Ophthalmology 88:583–600
5. Regnier S, Malcolm W, Allen F, Wright J, Bezlyak V (2014) Efficacy of anti-VEGF and laser photocoagulation in the treatment of visual impairment due to diabetic macular edema: a systematic review and network meta-analysis. PLoS One 9:e102309
6. Elman MJ, Aiello LP, Beck RW, Bressler NM, Bressler SB, Edwards AR, Ferris FL 3rd, Friedman SM, Glassman AR, Miller KM, Scott IU, Stockdale CR, Sun JK (2010) Randomized trial evaluating ranibizumab plus prompt or deferred laser or triamcinolone plus prompt laser for diabetic macular edema. Ophthalmology 117:1064–1077.e1035
7. Frisch GD, Shawaluk PD, Adams DO (1974) Remote nerve fibre bundle alterations in the retina as caused by argon laser photocoagulation. Nature 248:433–435
8. Watzke RC, Soldevilla JD, Trune DR (1993) Morphometric analysis of human retinal pigment epithelium: correlation with age and location. Curr Eye Res 12:133–142
9. Marshall J (1970) Thermal and mechanical mechanisms in laser damage to the retina. Investig Ophthalmol 9:97–115
10. Tababat-Khani P, Berglund LM, Agardh CD, Gomez MF, Agardh E (2013) Photocoagulation of human retinal pigment epithelial cells in vitro: evaluation of necrosis, apoptosis, cell migration, cell proliferation and expression of tissue repairing and cytoprotective genes. PLoS One 8:e70465
11. Pollack A, Korte GE (1990) Repair of retinal pigment epithelium and its relationship with capillary endothelium after krypton laser photocoagulation. Invest Ophthalmol Vis Sci 31:890–898
12. Romero-Aroca P, Reyes-Torres J, Baget-Bernaldiz M, Blasco-Sune C (2014) Laser treatment for diabetic macular edema in the 21st century. Curr Diabetes Rev 10:100–112
13. Strauss O (2005) The retinal pigment epithelium in visual function. Physiol Rev 85:845–881
14. Lee SH, Kim HD, Park YJ, Ohn YH, Park TK (2015) Time-dependent changes of cell proliferation after laser photocoagulation in mouse chorioretinal tissue. Invest Ophthalmol Vis Sci 56:2696–2708
15. Han JW, Lyu J, Park YJ, Jang SY, Park TK (2015) Wnt/beta-catenin signaling mediates regeneration of retinal pigment epithelium after laser photocoagulation in mouse eye. Invest Ophthalmol Vis Sci 56:8314–8324
16. Kim HD, Jang SY, Lee SH, Kim YS, Ohn YH, Brinkmann R, Park TK (2016) Retinal pigment epithelium responses to selective retina therapy in mouse eyes. Invest Ophthalmol Vis Sci 57:3486–3495
17. Rangarajan A, Weinberg RA (2003) Opinion: comparative biology of mouse versus human cells: modelling human cancer in mice. Nat Rev Cancer 3:952–959
18. Demetrius L (2005) Of mice and men. When it comes to studying ageing and the means to slow it down, mice are not just small humans. EMBO Rep 6 Spec No:S39–S44
19. Maeshima K, Utsugi-Sutoh N, Otani T, Kishi S (2004) Progressive enlargement of scattered photocoagulation scars in diabetic retinopathy. Retina 24:507–511
20. Chen Y, Hu Y, Zhou T, Zhou KK, Mott R, Wu M, Boulton M, Lyons TJ, Gao G, Ma JX (2009) Activation of the Wnt pathway plays a pathogenic role in diabetic retinopathy in humans and animal models. Am J Pathol 175:2676–2685
21. Zhang SJ, Li YF, Tan RR, Tsoi B, Huang WS, Huang YH, Tang XL, Hu D, Yao N, Yang X, Kurihara H, Wang Q, He RR (2016) A new gestational diabetes mellitus model: hyperglycemia-induced eye malformation via inhibition of Pax6 in the chick embryo. Dis Model Mech 9:177–186
22. Villarroel M, Garcia-Ramirez M, Corraliza L, Hernandez C, Simo R (2009) Effects of high glucose concentration on the barrier function and the expression of tight junction proteins in human retinal pigment epithelial cells. Exp Eye Res 89:913–920
23. von Leithner PL, Ciurtin C, Jeffery G (2010) Microscopic mammalian retinal pigment epithelium lesions induce widespread proliferation with differences in magnitude between center and periphery. Mol Vis 16:570–581
24. Kasaoka M, Ma J, Lashkari K (2012) c-Met modulates RPE migratory response to laser-induced retinal injury. PLoS One 7:e40771
25. Jain A, Blumenkranz MS, Paulus Y, Wiltberger MW, Andersen DE, Huie P, Palanker D (2008) Effect of pulse duration on size and character of the lesion in retinal photocoagulation. Arch Ophthalmol 126:78–85
26. Brem H, Tomic-Canic M (2007) Cellular and molecular basis of wound healing in diabetes. J Clin Invest 117:1219–1222
27. Alnek K, Kisand K, Heilman K, Peet A, Varik K, Uibo R (2015) Increased blood levels of growth factors, proinflammatory cytokines, and Th17 cytokines in patients with newly diagnosed type 1 diabetes. PLoS One 10:e0142976
28. Busik JV, Mohr S, Grant MB (2008) Hyperglycemia-induced reactive oxygen species toxicity to endothelial cells is dependent on paracrine mediators. Diabetes 57:1952–1965
29. Stojadinovic O, Brem H, Vouthounis C, Lee B, Fallon J, Stallcup M, Merchant A, Galiano RD, Tomic-Canic M (2005) Molecular pathogenesis of chronic wounds: the role of beta-catenin and c-myc in the inhibition of epithelialization and wound healing. Am J Pathol 167:59–69
30. Raviv S, Bharti K, Rencus-Lazar S, Cohen-Tayar Y, Schyr R, Evantal N, Meshorer E, Zilberberg A, Idelson M, Reubinoff B, Grebe R, Rosin-Arbesfeld R, Lauderdale J, Lutty G, Arnheiter H, Ashery-Padan R (2014) PAX6 regulates melanogenesis in the retinal pigmented epithelium through feed-forward regulatory interactions with MITF. PLoS Genet 10:e1004360
31. Ma X, Pan L, Jin X, Dai X, Li H, Wen B, Chen Y, Ma A, Qu J, Hou L (2012) Microphthalmia-associated transcription factor acts through PEDF to regulate RPE cell migration. Exp Cell Res 318:251–261
32. Torero Ibad R, Rheey J, Mrejen S, Forster V, Picaud S, Prochiantz A, Moya KL (2011) Otx2 promotes the survival of damaged adult retinal ganglion cells and protects against excitotoxic loss of visual acuity in vivo. J Neurosci 31:5495–5503
33. Housset M, Samuel A, Ettaiche M, Bemelmans A, Beby F, Billon N, Lamonerie T (2013) Loss of Otx2 in the adult retina disrupts retinal pigment epithelium function, causing photoreceptor degeneration. J Neurosci 33:9890–9904
34. Tamiya S, Liu L, Kaplan HJ (2010) Epithelial-mesenchymal transition and proliferation of retinal pigment epithelial cells initiated upon loss of cell-cell contact. Invest Ophthalmol Vis Sci 51:2755–2763
35. Scoles D, Sulai YN, Dubra A (2013) In vivo dark-field imaging of the retinal pigment epithelium cell mosaic. Biomed Opt Express 4:1710–1723
36. Burns SA, Elsner AE, Sapoznik KA, Warner RL, Gast TJ (2018) Adaptive optics imaging of the human retina. Prog Retin Eye Res
37. Datta R, Alfonso-Garcia A, Cinco R, Gratton E (2015) Fluorescence lifetime imaging of endogenous biomarker of oxidative stress. Sci Rep 5:9848
38. Dysli C, Wolf S, Berezin MY, Sauer L, Hammer M, Zinkernagel MS (2017) Fluorescence lifetime imaging ophthalmoscopy. Prog Retin Eye Res 60:120–143